

SULFUR SOLUBILITY IN BASALTS FROM THE NORTHERN VOLCANIC PLAINS OF MERCURY.

Olivier Namur¹ and Bernard Charlier¹; ¹Institute of Mineralogy, University of Hannover, Germany (o.namur@mineralogie.uni-hannover.de)

Introduction: A peculiar feature of lavas at the surface Mercury is their very high sulfur concentrations (~1-4 wt.% S; [1]). This is unique in terrestrial planets and understanding the sulfur solubility and speciation in Mercury's silicate melts will help deciphering global differentiation processes of the planet.

Based on MESSENGER imaging, Mercury's surface can be subdivided into two major units: (1) the heavily cratered terrains and (2) the smooth plains, occupying ca. 40% of the Mercury's surface [2]. A significant proportion of the smooth plains covers much of the Mercury's high northern latitudes and occupies more than 6% of the planet's surface area [3]. This area, called Northern Volcanic Plains (NVP), is considered as having emplaced in a similar way to flood-basalt on Earth and its global composition is intermediate between basalts and komatiites [4].

In this project, available data for surface composition of the Mercury's NVP are used to calculate absolute abundances of major elements for surface materials. The NVP probably represent the most homogeneous magmatic unit in composition at the surface of Mercury. We present results of low to medium pressure experiments (surface and lower crust) and investigate the sulfur solubility in silicate melts under the reducing conditions of Mercury. These results are used to determine whether the high-S concentrations observed at the surface of the planet can be explained by high S-solubility in silicate melts or, alternatively, if they point to accumulated sulfide minerals.

Starting composition: We used XRS data for Mg/Si, Al/Si, Ca/Si ratios from 45 footprints in the NVP to calculate absolute composition for SiO₂, MgO, Al₂O₃ and CaO [5]. We performed some statistical tests to get constraints on the geochemical variability (see Figure 1) of these rocks and we used the median value of each ratio to get a representative composition for the whole NVP. We also considered that lavas from the NVP contain 0.5 wt.% TiO₂ [1,5], 7 wt.% Na₂O [6] and 0.2 wt.% K₂O [7]. For minor elements, we used data from terrestrial komatiites with average values of 0.1 wt.% Cr₂O₃, NiO, and MnO. We then renormalized the composition to a total of 100 wt.% and used this calculated composition (Table 1) as the starting composition for experiments.

Experimental procedure: The starting composition was prepared by mixing high-purity oxides and silicates. Sulfur was added either as S or as FeS. Sufficient sulfur (at least 15 vol.%) was added to the starting composition to ensure sulfide saturation in each

experiment. Most experiments were performed at 1 and 3 kbar in large-volume internally heated pressure vessels using argon as a pressure medium. The starting composition (ca. 50 mg) was placed in graphite or forsterite capsules with a Pt outer jacket welded shut. Experiments were run for 8 hours at 1250 and 1300°C. Another set of experiments was performed in a 1-atm gas mixing furnace. The starting composition (ca. 50 mg) was placed in graphite or forsterite capsules enclosed into an evacuated silica tube. In some experiments, a crucible with albite was added as an external source for Na. Experiments were run for 1-3 hours at 1300°C.

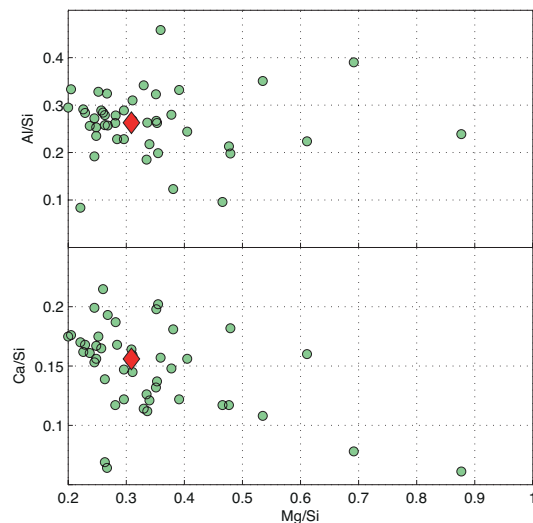


Figure 1: XRS data (green spots) from [3] for surface composition of Mercury's North Volcanic Plains plotted for Al/Si and Ca/Si as a function of Mg/Si mass. Red diamonds show the starting composition used for experiments.

Control on oxygen fugacity: Oxygen fugacity conditions on Mercury are expected to range from IW-2 to IW-7 (with IW corresponding to the iron-wustite buffer; [8,9]). In IHPV experiments, this range of oxygen fugacity was reached by adjusting the Si/SiO₂ ratio of the starting composition by adding Si metal to oxide and silicate mixture [10]. Detailed thermodynamic treatment has still to be performed [11] but according to other experimental studies, we can estimate that our experiments were performed at ~ IW (0% Si metal), [10,12], IW-4 to IW-6 (5-20% Si metal) and IW-7 (50% Si metal; [13]). In 1-atm experiments, the oxygen fugacity was controlled by using external solid buffers such as Fe/FeO (IW), Cr/Cr₂O₃ (IW-4) and Ta/Ta₂O₅ (IW-7).

Results:

Phase relationships – High temperature runs (1300-1310°C) are generally near-liquidus experiments, with a large proportion of silicate melt. Other phases include a few crystals of pure forsterite and one or several immiscible metal melts. Metal melts may include (1) a FeSi-rich melt, (2) a FeS-rich melt and (3) a CaMgS-rich melt. At lower temperature (1250°C), phase relationships are identical but the proportion of forsterite crystals is significantly higher.

Composition of the silicate melt – The S content of the melt shows a correlation with the oxygen fugacity conditions. The sulfur solubility is relatively low (~0.5 wt.%) near the IW buffer, and increases significantly with reducing conditions (2-4 wt.%; IW-4 to IW-6). Another interesting observation is the TiO₂ content of the silicate melt which seems to drop significantly in the most reduced runs. No obvious dependence of the pressure conditions on the S solubility was observed.

Table 1: Starting composition and experimental results

	(1)	(2)	(3)	(4)	(5)
Pressure (kbar)	-	1	1	1	1
Temp	-	1310	1310	1310	1310
Ox Fugacity	-	IW	IW-4	IW-5	IW-6
SiO ₂	56.56	58.06	58.85	56.00	54.40
TiO ₂	0.50	0.50	0.40	0.43	0.08
Al ₂ O ₃	13.28	13.80	12.17	13.13	13.79
Cr ₂ O ₃	0.10	0.01	0.01	0.02	0.01
FeO	-	0.47	0.11	0.02	0.02
MnO	0.20	0.06	0.08	0.12	0.13
MgO	13.46	11.24	12.30	13.13	13.90
CaO	5.61	5.98	5.74	5.81	5.98
Na ₂ O	7.01	7.78	7.48	7.66	8.02
K ₂ O	0.08	0.09	0.09	0.12	0.09
S	-	0.50	2.01	3.07	3.92

(1) Starting composition; (2-5) Representative experimental melts

Composition of the metal melts – Representative composition of these melts are given in Table 2. The FeS- and FeSi-rich melts are by far the most abundant. The composition of the FeS- and CaMgS-rich melts is relatively stable for major elements but may significantly change for minor elements (Ni, Cr, Mn) as a function of oxygen fugacity conditions. The Fe/Si ratio of the FeSi melt is also strongly dependent on the oxygen fugacity conditions with a strong increase of the Si-content under highly reduced conditions. No obvious compositional dependence with pressure was observed.

Discussion and future work:

Available experimental results can be compared with the sulfur content observed in NVP rocks at the surface of Mercury. It can be seen from Figure 2 that the S-content in NVP rocks range from 0.5 to 3 wt.%. This range is relatively similar to the values of sulfur

solubility in the silicate melt observed in the experiments. This may indicate that the basalts of Mercury's

Table 2: Composition of metal melts

Pressure (kbar)	1	1	1
Temp	1310	1310	1310
Ox Fugacity	IW-4	IW-4	IW-4
	FeS	CaMgS	FeSi
Si	0.02	0.02	7.27
Ti	3.37	0.94	0.00
Fe	55.18	7.93	90.83
Mn	0.68	2.70	0.03
Mg	0.11	7.85	0.00
Ca	0.59	35.90	0.04
Cr	3.15	0.29	0.09
Ni	1.36	0.06	1.73
S	35.53	44.31	0.00

NVP may have not reached sulfide-saturation at the liquidus temperature and the sulfur at the surface of Mercury may be comprised in sulfide minerals having crystallized from immiscible melts exsolved during cooling and crystallization. Given the low

Fe-content at the surface of Mercury, it is likely that most of the sulfide minerals are from the oldhamite (CaS) – niningerite (MgS) solid solution and that they crystallized from a Mg-Ca-S-rich melt (Table 2). Our experimental results furthermore indicate that the Mg/Ca-ratio of such a melt may be highly variable and possibly linked to the oxygen fugacity conditions.

Future work includes (1) a detailed comparison of experimental products performed in graphite and forsterite capsules; (2) a comparison of experimental products with only S or FeS in the starting composition; (3) an investigation of sulfur solubility at high pressure (5-40 kbar) and (4) a detailed investigation of the role of oxygen fugacity, pressure and temperature on the major and trace element partitioning between the silicate melt and the metal melts. We will especially investigate how changing the oxygen fugacity conditions controls the major element composition of the CaMgS melt.

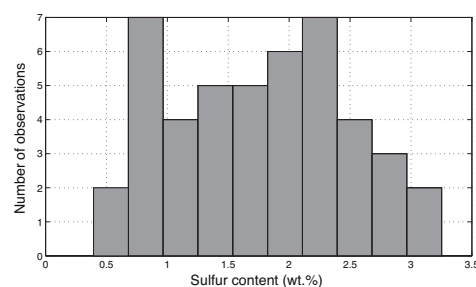


Figure 2: Histogram showing the range of S-content observed in rocks from the NVP. Data are recalculated from [3].

References: [1] Nittler et al (2011) *Science* 333, 1847-1850. [2] Denevi et al. (2013). *JGR* 118, 891-907. [3] Denevi et al (2009) *Science* 324, 613-618. [4] Head et al (2011) *Science* 333, 1853-1856. [5] Weider et al (2012) *JGR Planets* 117. [6] Peplowski et al (2014) *Icarus* 228, 86-95. [7] Peplowski et al (2012) *JGR Planets* 117. [8] Malavergne et al (2010) *Icarus* 206, 199-209. [9] McCubbin et al (2012) *GRL* 39. [10] Berthet et al (2009) *GCA* 73, 6402-6420. [11] Corgne et al (2008) *GCA* 72, 574-589. [12] Arculus et al (1990) In: Newsom & Jones, Origin of the Earth. Oxford University Press, 251-271. [13] Malavergne et al (2004) *GCA* 68, 4201-4211.